Tetrahedron 67 (2011) 7222–7230

Contents lists available at ScienceDirect

Tetrahedron

journal homepage: www.elsevier.com/locate/tet

Influence of solvent on the thermal stability and organization of self-assembling fibrillar networks in methyl-4,6-*O*-(*p*-nitrobenzylidene)-α-D-glucopyranoside gels

M. Bielejewski [a], A. Łapiński [a], R. Luboradzki [b], J. Tritt-Goc [a,*]

[a] Institute of Molecular Physics, Polish Academy of Sciences, ul. M. Smoluchowskiego 17, 60-179 Poznań, Poland
[b] Institute of Physical Chemistry, Polish Academy of Sciences, ul. Kasprzaka 44/52, 01-224 Warsaw, Poland

ARTICLE INFO

Article history:
Received 24 March 2011
Received in revised form 27 June 2011
Accepted 21 July 2011
Available online 28 July 2011

Keywords:
Sugar-based gelator
Self-assembling
Gel microstructure
Gel stability
Solvents influence

ABSTRACT

Sugar based low-molecular-mass organogelator (LMOG) methyl-4,6-*O*-(*p*-nitrobenzylidene)-α-D-glucopyranoside, is a unique gelator because its small and weakly-interacting molecules can form large supramolecular structures in nonpolar, but also in polar, solvents and cause their gelation. The self-assembling properties of the gelator were studied in selected nonpolar and polar solvents. It was shown that the driving forces for both types of solvent are the intermolecular hydrogen bond interaction. The effect of the nature of the solvent on the thermal stability of the gels and on the three-dimensional network organization was determined. Different solvent parameters, such as dielectric constant, one-component solubility parameter, the polarity parameter and the Kamlet–Taft parameters were considered to quantify solvent effects on the gelation. Some correlation between these parameters and the gel stability, microstructure and the enthalpy of the phase transition were established. The effort to correlate the Kamlet–Taft parameters to the thermal stability and gelation ability is also possible but applies only to the studied gelator.

1. Introduction

Methyl-4,6-*O*-(*p*-nitrobenzylidene)-α-D-glucopyranoside (**1**) belongs to the family of monosaccharides that are still not fully explored. Moreover, it is the representative of so-called low-molecular-mass (LMOGs) or low-molecular-weight (LMWGs) sugar-based gelators.[1–6] The characteristic feature of all LMOGs is that they gelate various organic solvents and create a novel fibrous superstructure.[7–17] On the base of the studies conducted on the gels made by LMOGs it is generally accepted that the gelator and the solvent molecules form a homogeneous mixture in the sol phase. At the sol-gel temperature they separate into two phases: the solid fibril like structure formed by the gelator aggregates and the liquid one confined within the pores, spaces of the solid matrix. Gelator molecules in the fibers are self-assembled through non-covalent interactions, such as electrostatic, dipole–dipole, hydrogen bonding, the π–π stacking, and van der Waals interactions. Therefore the gels made by LMOGs are classified as physical gels. An interesting feature of the LMOG gel is that even up to 99.5% of the gel by weight is liquid.

The organogels represent an important class of functional materials due to their interesting supramolecular architectures and potential applications in template materials, biomimetics, as viscosity modifiers in applications such as paints, coatings, oil recovery, in controlled drug release and in a variety of pharmaceutical and hygienic applications.[3,7,10,11]

Despite a variety of studies of the gelation process, our understanding of the gel formation remains incomplete and some questions still remain. The most important are: how the gelator molecules assemble step by step into aggregates and further into complicated microstructures, how the solvent influences the gel properties, and how the solvent molecules interact with the gelator aggregates in gel, if such an interaction takes place.

In our work we focus on the gelation phenomenon of saccharide gelators.[18–20] In particular we are interested in the thermal properties, microstructure and solvent–gelator interactions. The saccharide gelators create in the solid state one-dimensional hydrogen-bond-based chains that are the buildings blocks of the fibril-like gelator structure in the gel.[21–23] The tendency to form one-dimensional hydrogen-bonded networks is a prerequisite for a good gelator. Usually a particular gelator, which gels a large spectrum of organic solvents, does not act as a gelator for polar solvents like water or alcohols. Why is that so? The driving forces for the aggregation of gelator molecules are intermolecular hydrogen bonds. Polar solvents can usually form hydrogen bonds with gelator molecules competing with the gelator–gelator hydrogen bond formation.

The subject of our studies, methyl-4,6-*O*-(*p*-nitrobenzylidene)-α-D-glucopyranoside, is a unique gelator, not only in the family of sugar-based gelators, but also in the large group of LMOGs because

* Corresponding author. Tel.: +48 061 8695 226; e-mail address: jtg@ifmpan.poznan.pl (J. Tritt-Goc).

0040-4020/$ – see front matter © 2011 Elsevier Ltd. All rights reserved.
doi:10.1016/j.tet.2011.07.071

its small and weakly-interacting molecules can form large supramolecular structures both in nonpolar and polar solvents and cause their gelation. The most plausible conformation of the methyl-4,6-*O*-(*p*-nitrobenzylidene)-α-D-glucopyranoside obtained by computational chemistry methods is shown in Fig. 1. The ability to form gel with a polar solvent is of great importance due to many potential applications in the biomedical field, including tissue engineering, controlled drug release or medical implants.[24,25] These 'bifunctional' gelators are limited in the literature.[14,26]

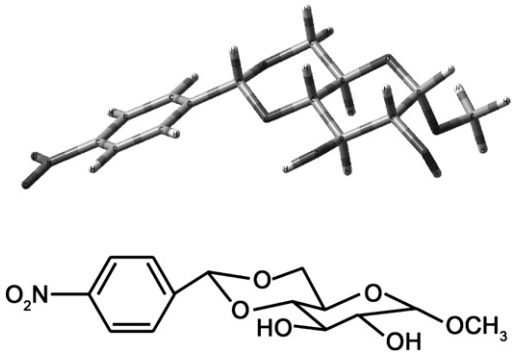

Fig. 1. The most possible conformation of the methyl-4,6-*O*-(*p*-nitrobenzylidene)-α-D-glucopyranoside obtained by computational chemistry methods.

Unfortunately, the crystal structure for the studied gelator is unknown but it is reasonable to assume that it is very similar to the methyl-4,6-*O*-benzylidene-α-D-glucopyranoside.[21,22] The studied gelator differs only by the nitro group attached to the benzylidene in the *para*-position. In the crystal state, the non-substituted gelator forms one-dimensional zigzag chains in which molecules are connected by two intermolecular hydrogen bonds using the hydroxyl group 2-OH and 3-OH. It was shown that the introduction of a nitro-substituent in the *para*-position increases the ability for self-aggregation of methyl-4,6-*O*-benzylidene-monosaccharides.[24]

In the former contribution we focused on the solvent–gelator interaction in the gel composed by the methyl-4,6-*O*-(*p*-nitrobenzylidene)-α-D-glucopyranoside with chlorobenzene.[20] The interaction was evidenced through the proton spin-lattice relaxation measurements of chlorobenzene as a function of magnetic field and temperature. The interactions of the chlorobenzene molecules with the surface of gelator aggregates, which formed the solid fibril networks in the gel are responsible for the observed dispersion of the relaxation of the solvent in the frequency range 10^4–10^5 Hz.

This paper deals with the gelation of polar and nonpolar solvents by the methyl-4,6-*O*-(*p*-nitrobenzylidene)-α-D-glucopyranoside. We study the effect of the nature of the solvent on the thermal stability of the gels, on the three-dimensional network organization, and on the interactions responsible for the self-assembly of the gelator molecules.

2. Results and discussion

2.1. Gelation properties and the thermal stability of the gels

The gelation ability of gelator **1** was examined in six different nonpolar and polar solvents, such as toluene, benzene, chlorobenzene, butanol, glycerol, and water. The results are summarized in Table 1. Gelator **1** is able to form stable gels (classified as G) in all of these solvents, but at different minimum concentration. With toluene, benzene, and chlorobenzene gelator **1** makes gels at a concentration of 0.5%, whereas with butanol the minimal concentration is 3% [wt %].

The physical gelation of **1**, like with other LMOGs, occurs via self-aggregation through non-covalent interactions. Therefore, the thermally reversible gel-to-sol phase transition is a characteristic feature of the gels. In order to compare the qualities of the gels composed by **1** with the studied solvents, the gel–sol phase transition temperatures (T_{gel}) are plotted against the gelator concentration (in wt %) and presented in Fig. 2 A. The temperatures were estimated by the air-bath method.[6] The T_{gel} value is dependent on

Table 1
Gelation ability of **1** in studied solvents

Non-polar polar aprotic solvents									
	0.5% (wt %)	1.0% (wt %)	1.5% (wt %)	2.0% (wt %)	2.5% (wt %)	3.0% (wt %)	4.0% (wt %)	5.0% (wt %)	6.0% (wt %)
Toluene	G	G	—[a]	G	—[a]	G	G	I	—[a]
Benzene	G	G	G	G	I	I	—[a]	—[a]	—[a]
Chlorobenzene	G	G	—[a]	G	—[a]	G	G	I	—[a]
Polar protic solvents									
1-Butanol	S	P	P	P	P	G	G	G	G
Glycerol	S	S	G	G	G	G	G	I	—[a]
Water	S	S	G	G	—[a]	G	G	G	I

G=gel, P=precipitation, S=solution, I=insoluble.
[a] Not measured.

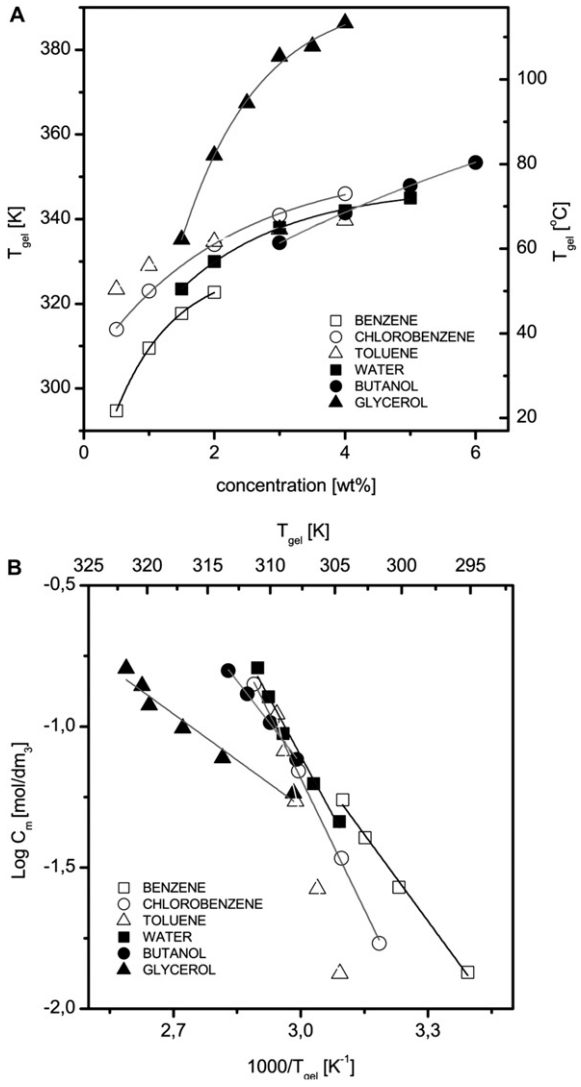

Fig. 2. (A) Dependence of T_{gel} on the concentration of gelator **1** gels in benzene (open squares), chlorobenzene (open circles), toluene (open triangles), water (filled squares), butanol (filled circles), glycerol (filled triangles). The solid lines have no physical meaning and are included as a visual guide. (B) Plots of the logarithm of gelator **1** concentration versus the reciprocal absolute temperature of T_{gel}. The solid lines are the best fit of Eq. 1 to the experimental points.

the concentration of the gelator and in agreement with the literature, in all investigated gels increased with increasing gelator concentration. The data showed that for the concentration of 2% [wt %] the T_{gel} of **1** gels increase in the order of **1**/benzene<**1**/water<**1**/chlorobenzene<**1**/toluene, <**1**/glycerol, corresponding to the increasing polarity of the solvent. The polar protic glycerol produced the most thermally stable gel with **1**.

The saccharide based gelators[1,2,21] form fibril aggregates in the gel state whereas the aggregates are dissociated into discrete molecules of gelator in the sol phase. Therefore, the gel-to-sol phase transition can be treated like the dissolution process of the crystal and if so, the transition temperature and its relation to the gelator concentration is described by Eq. 1 derived from a Schrader's[27] relation.

$$\log[C] = -\frac{\Delta H}{2.303R} \times \frac{1}{T_{gel}} + \text{constant} \quad (1)$$

where C is the gelator concentration, ΔH is the melting enthalpy, R is the gas constant and T_{gel} is the gel-to-sol transition temperature.

Eq. 1 was originally proposed for the gel-to-sol phase transition for polymeric networks whose crosslink formation is made up of pairs of chains and does not take into account the influence of the solvent, which may affect the structures and thermodynamic behaviors.[28] Therefore, using Eq. 1 for describing the physical gel is probably oversimplified but is generally accepted and was used to fit the experimental data of the gelator concentration versus the reciprocal absolute temperature of T_{gel}. The best fits are shown as the solid lines in Fig. 2B. The determined gel–sol transition enthalpies ΔH are presented in Table 2.

Table 2
Bulk solvent parameters of the six selected solvents: ε=dielectric constant, δ=one-component solubility parameter, $E_T(30)$=polarity parameter and the Kamlet–Taft parameters: α=hydrogen bond donor ability, β=hydrogen bond acceptor ability, and π^*=solvent dipolarity/polarisability. The T_{gel} is the gel–sol temperature obtained for 3% [wt %] studied gels and ΔH is the enthalpy calculated on the base of Eq. 1

Non-polar and polar aprotic solvents								
	ε	δ (cal$^{1/2}$ cm$^{-3/2}$)	$E_T(30)$ (kcal mol^{-1})	α	β	π^*	T_{gel} (K)	ΔH (kJ mol^{-1})
Toluene	2.4	8.9	33.9	0.00	0.11	0.54	337.6	117.9
Benzene	2.3	9.1	34.3	0.00	0.10	0.59	327.8	39.2
Chlorobenzene	5.6	9.6	36.8	0.00	0.07	0.71	341.0	59.3
Polar solvents								
Butanol	17.8	11.3	49.9	0.79	0.88	0.47	334.4	37.4
Glycerol	42.5	21.1	57.0	0.93	0.67	1.04	378.4	20.9
Water	80.0	23.5	63.1	1.17	0.18	1.09	338.0	53.2

The obtained values fit well with the values reported up to now for the other monosaccharide based gels.[5,6,29] As the ΔH values are relative to the strength of the intermolecular interactions (mainly hydrogen bonding) in the nanofiber, the highest ΔH value in the toluene gel of **1** reflects the stronger intermolecular interactions. This result is consistent with our FTIR measurements as discussed below.

2.2. Mechanism of gelator aggregates

The FTIR spectra for the solid gelator methyl-4,6-*O*-(*p*-nitrobenzylidene)-α-D-glucopyranoside and its gels were measured to examine the participation of hydrogen bonding in gelation. FTIR spectra give valuable information about the formation of hydrogen bonding because the stretching vibrations ν_{OH} along the bond linking atoms or groups of atoms are strongly affected by this type of interactions. Generally, in FTIR spectra of solid samples (KBr) of all monosaccharides the peak for free OH group appears around 3600 cm^{-1}. In the gel phase all signals are broadened and those involved in intermolecular hydrogen bonds are shifted toward lower wave number.

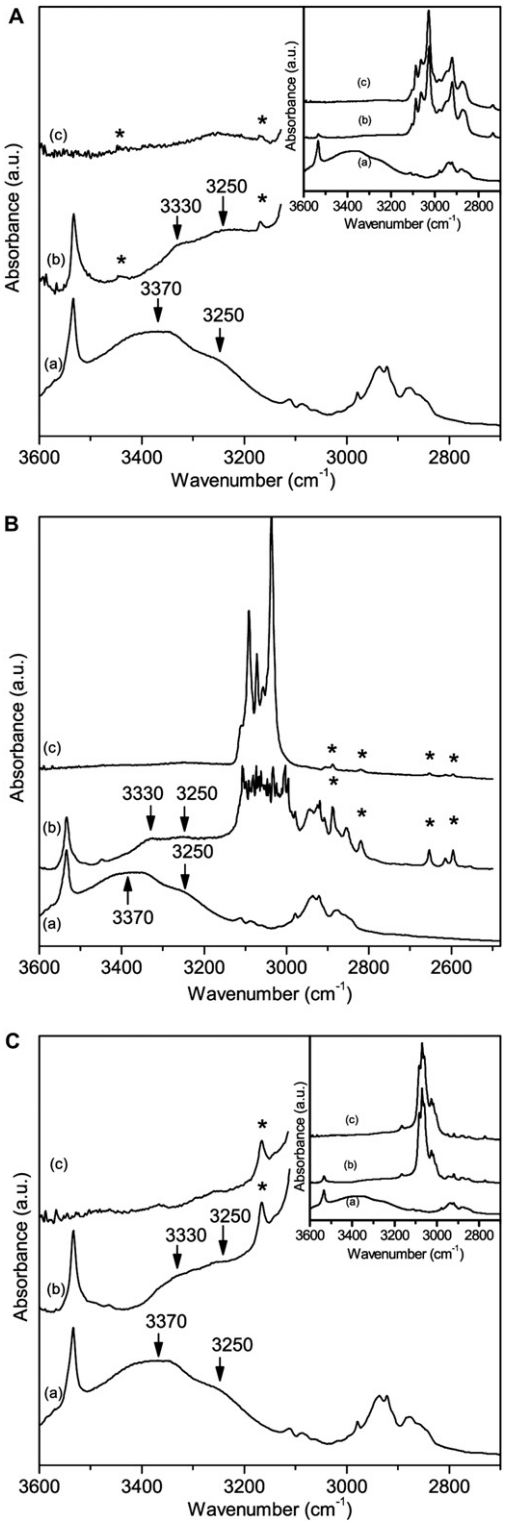

Fig. 3. Selective part of the absorption FTIR spectra of gelator **1** for toluene (A), benzene (B) and chlorobenzene (C) gels. In each of the figures the spectra are shown of the solid gelator **1** (a), corresponding gel (b), and solvent (c). The stars indicate the signal form solvent.

In Fig. 3A, B, and C are shown the FTIR spectra of nonpolar solvent: toluene, benzene, and chlorobenzene gels (b) together with the spectra of the solid gelator **1** (a), and corresponding

solvents (c). The measured spectra of solid gelator **1** and gels are characterized by the bands in the range of 3600–3100 cm^{-1} attributed to intermolecular hydrogen bonding. Below 3500 cm^{-1} a broad intense band (3500–3100 cm^{-1}) with two distinguishable peaks at 3370 and 3250 cm^{-1} is seen in the solid phase. These two peaks can be connected with gelator hydroxyl group 2-OH and 3-OH, which formed two intermolecular hydrogen bonds between gelator molecules giving contribution to the one-dimensional zig-zag chains observed in the crystal.[21,22] In the gel phase (for toluene, benzene, and chlorobenzene) the broad band also appears but its intensity decreases, the signal is more broadened and the ν_{OH} peak at 3370 cm^{-1} changes its position to 3330 cm^{-1}. The shifts of 40 cm^{-1} for gel state indicate involvement of only one of the OH groups in intermolecular H-bonding during gel assembly. Moreover, the broad band in the solid and gel phase indicates distribution of the intermolecular hydrogen bonds. In the discussed FTIR spectra, in addition to a broad band, a strong, narrow peak also appears at 3534 cm^{-1} in solid and gel phases with the same intensity. Its position corresponds approximately to the position of the peak from a free OH group. We assigned this peak to the weak intramolecular hydrogen bond formed between 2-OH group and the 1-*O*-Me group of the gelator molecule, which is not affected by the gelation process.

The interesting feature of the FTIR spectra of gelator **1** with toluene, benzene and chlorobenzene gels is their similarity, which may reflect comparable hydrogen bond networks. However, a close look at the peak at 3250 cm^{-1} reveals some differences. The position of this peak is independent of the solvent but its intensity is strongly influenced by the solvent. Therefore, we compare the relative intensities of the peak at 3250 cm^{-1} to the one at 3534 cm^{-1} (the position and the intensity of this peak remains unchanged in solid and in the gels) in the spectra of benzene, chlorobenzene, and toluene gels. The differences in the intensities are 0.28, 0.30, and 0.16, for benzene (Fig. 3B), chlorobenzene (Fig. 3C), and toluene (Fig. 3A), respectively. The result indicates almost twice as many hydrogen bonds in the gel of gelator **1** with toluene as compared with benzene or chlorobenzene. The result is consistent with the determined gel–sol transition enthalpies ΔH with the highest value being observed for toluene gel.

Fig. 4A, B shows the FTIR spectra of polar solvent: water and glycerol gels (b) together with the spectra of the solid gelator **1** (c), and corresponding solvents (a). The polar solvents are composed of the OH group therefore their FTIR spectra are characterized by the strong band in the range of 3500–2800 cm^{-1} attributed to hydrogen bonding. This makes the gel spectra, due to the dominant solvent contribution, very like the solvent spectra. The identification of the peaks assigned to the OH groups of the gelator involved in the hydrogen bond formation is impossible. In the case of water and glycerol the only observation from FTIR spectra concerns the broadening of the band in gels as compared to the solid gelator or solvents. The result indicates the formation of additional hydrogen bonds and their broader distribution in the gel phase. The polar solvent can form hydrogen bonds with gelator molecules in addition to the gelator–gelator hydrogen bonds formation (unidirectional) and thus stimulate the growth of hydrogen bonds in all directions. The analysis of the FTIR spectra in the range of 1800–800 cm^{-1} does not show significant involvement of any other interaction in the gel formation.

As shown by Polarized Optical Microscopy, the butanol gel of gelator **1** contrary to other studied gels formed three different fibril microstructures (Fig. 11). Therefore, FTIR measurements were performed for each part of the gel with a different structure. Corresponding spectra are presented in Fig. 5A and B in the range ascribed to hydrogen bonding and the lower wave number range (1550–800 cm^{-1}), respectively. On both figures are presented

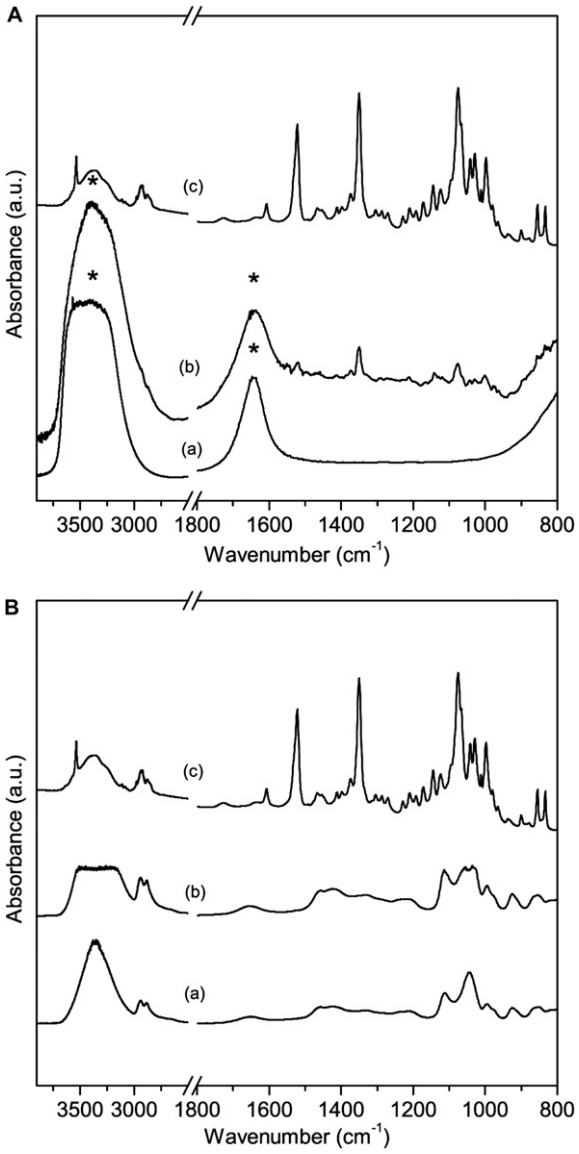

Fig. 4. Absorption FTIR spectra of water (A) and glycerol (B) gels of gelator **1**. In both figures the spectra are shown for solvents (a), corresponding gel (b) together with the spectra of the solid gelator **1** (c). The stars indicate the signal form solvent.

spectra from butanol (a), the part of the gel, which showed a branch-like aggregates structure (b), the part of gel in which the aggregates exist in the form of straight fibers (c), the part of the gel with aggregates exhibited tussock grass-like structure (d), and the spectra of the solid gelator **1** (e). We can see some differences between the FTIR spectra of different aggregates in the studied range between 3600 and 800 cm^{-1}. In the range assigned to the hydrogen bonds the spectra from particular aggregates show differences between each other and also they differ from that of a solid gelator and solvent. The result shows that despite the fact that the polar solvent can compete with the gelator–gelator hydrogen bonds formation the hydrogen-bond interaction still remains a driving force for gel formation. In the FTIR spectra of gel with aggregates in the form of straight fibers and branch-like aggregates the ν_{OH} peaks change their position to 3300 cm^{-1} and 3160 cm^{-1} as compared to the peaks in solid gelator, which appear at 3370 cm^{-1} and 3250 cm^{-1}. The shifts of 70 cm^{-1} and 90 cm^{-1} for the gel state indicate the involvement of both OH groups of the gelator in intermolecular H-bonding during gel assembly.

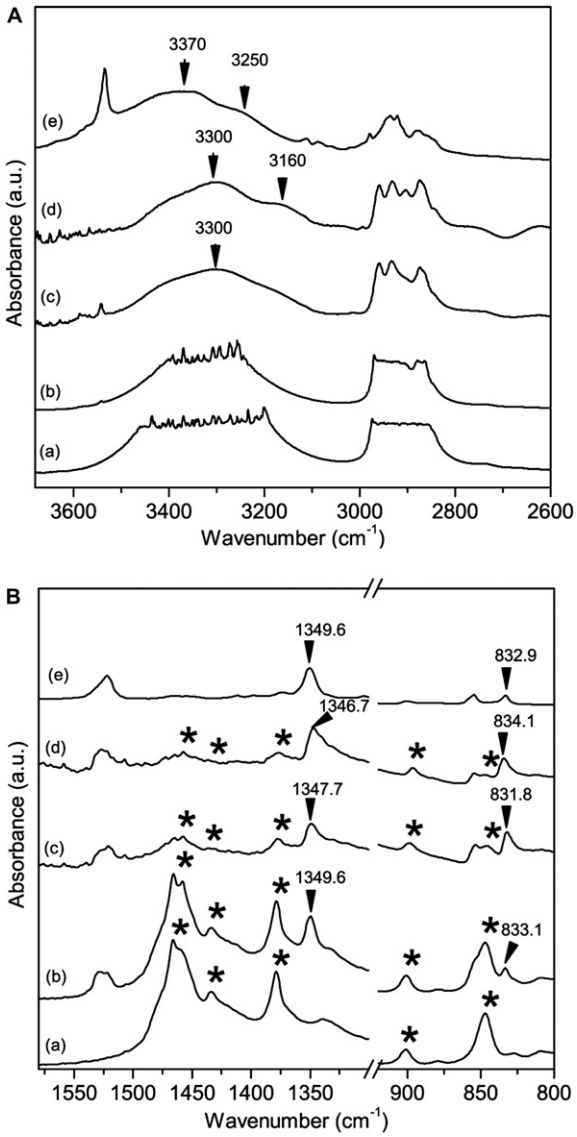

Fig. 5. Absorption FTIR spectra of **1** for butanol gel in the range ascribed to hydrogen bonding (A) and in the lower wave number range 1550–800 cm^{-1} (B). On both figures spectra are presented from butanol (a), the part of the gel, which showed a branch-like aggregates structure (b), the part of gel in which the aggregates exist in the form of straight fibers (c), the part of the gel with aggregates exhibited tussock grass-like structure (d), and the spectra of the solid gelator **1** (e). The stars indicate the signal form the solvent.

The interesting feature of butanol gels and other studied polar solvents is the absence of a peak at 3530 cm^{-1} assigned to the weak intramolecular hydrogen bond formed between the 2-OH and 1-*O*-Me group of gelator molecule in solid phase. Inversely to nonpolar solvents this interaction is affected by the gelation process.

FTIR spectra in the range of the lower wave number also show some differences. In butanol one intensive and narrow peak at 850 cm^{-1} is detected. This peak, but with different intensity, is also visible in the gels with different microstructure (b, c, and d) together with the peak around 830 cm^{-1} assigned to the gelator **1**. The analysis of the intensity of these two peaks in the gel with microstructure b, c, and d leads to the following conclusion: the different aggregates interact with different number of butanol molecules as a result of a different value of the surface area of the aggregates. In the case of a branch-like aggregates (b) characterized by the highest surface area, the peak from butanol at 850 cm^{-1} has higher intensity when compared to the one at 833.1 cm^{-1} assigned to the gelator (see Fig. 6b). On the other hand for aggregates in the form of straight fibers (c) the situation is reversed and the peak at 831.8 assigned to the gelator is more intense than the one at 850 cm^{-1} assigned to solvent. This means that straight fiber aggregates are characterized by the smaller surface area for the solvent–gelator interaction as compared to branch-like aggregates. In the FTIR spectra of the gelator **1** the peak at 1349.6 cm^{-1} corresponds to stretching vibration of CN where N belongs to NO_2 group. This peak is shifted toward the lower wave number for gels with straight fibers and tussock grass-like aggregates (1347.7 and 1346.7, respectively) indicating possible involvement of NO_2 in the formation of aggregates and in gelation phenomenon.

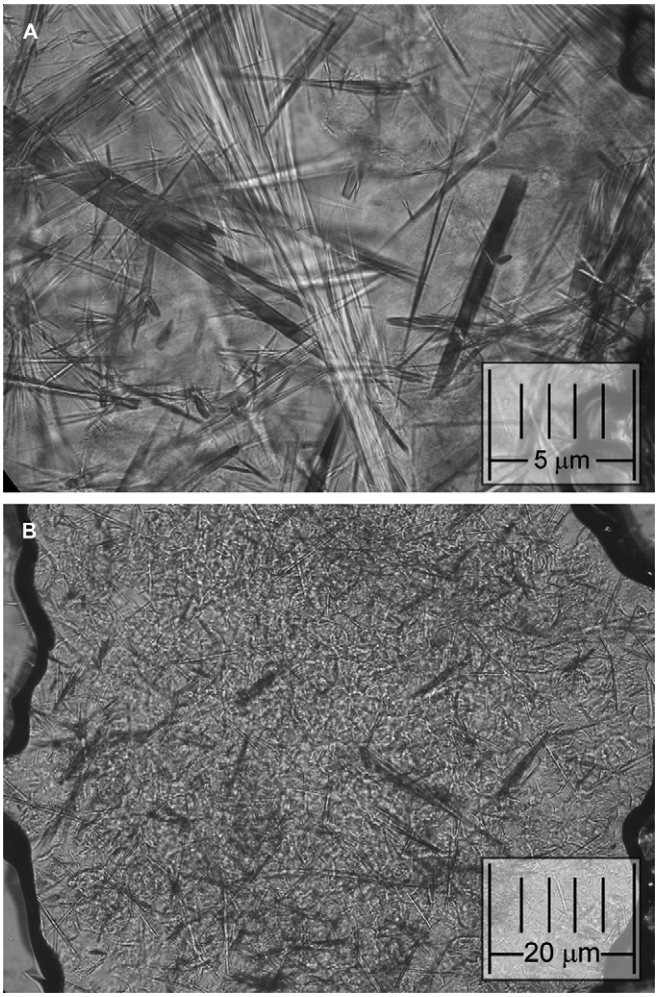

Fig. 6. Polarized Optical Microscopy micrographs of toluene gel **1** [2%(wt%)]: high magnification (A) and low magnification (B).

FTIR studies show that gelator **1**, like other methyl-4,6-*O*-benzylidene derivatives of monosaccharides,[30,31] formed gels in nonpolar: toluene, benzene, and chlorobenzene and in polar solvents: butanol, through formation of a hydrogen-bond network. Due to the unresolved FTIR spectra of water and glycerol gels we are unable to determine the role of hydrogen-bonds interactions. Based on the literature[14,26] we can assume that other aggregation modes, such as dipole–dipole, hydrophobic or the π–π stacking interactions may play some minor role in the self-assembly of gelator **1** in the polar solvents. The π–π interactions were detected in FTIR spectra of butanol gel.

2.3. Gel structure

The morphology of gels produced by methyl-4,6-*O*-(*p*-nitrobenzylidene)-α-D-glucopyranoside with studied solvents was examined by Polarized Optical Microscopy (POM). Representative micrographs are shown in Figs. 6–11 where the structure of a particular gel is presented with low and high magnification. The POM images were taken of 2% gels in the case of toluene, benzene, chlorobenzene, water, and glycerol and 3% for the butanol gel. They show clear differences in the morphology of gelator **1** in different solvents. The aggregates have very different shapes for each of the solvent. In the case of toluene they have short but thick, needle fiber shape but change into the long puckered fibrils in water. An image of **1** in chlorobenzene exhibited branch-like structure at low magnification, slightly similar to the one of benzene but at high magnification. Contrary to the others gels, the gel of **1** with butanol has different fibril microstructure (Fig. 11A). One type of aggregates showed a branch-like structure (Fig. 11b), which clearly has one starting point of growing, the second type exists in the form of straight fibers (Fig. 11c), and the third one exhibited tussock grass-like structure (Fig. 11d).

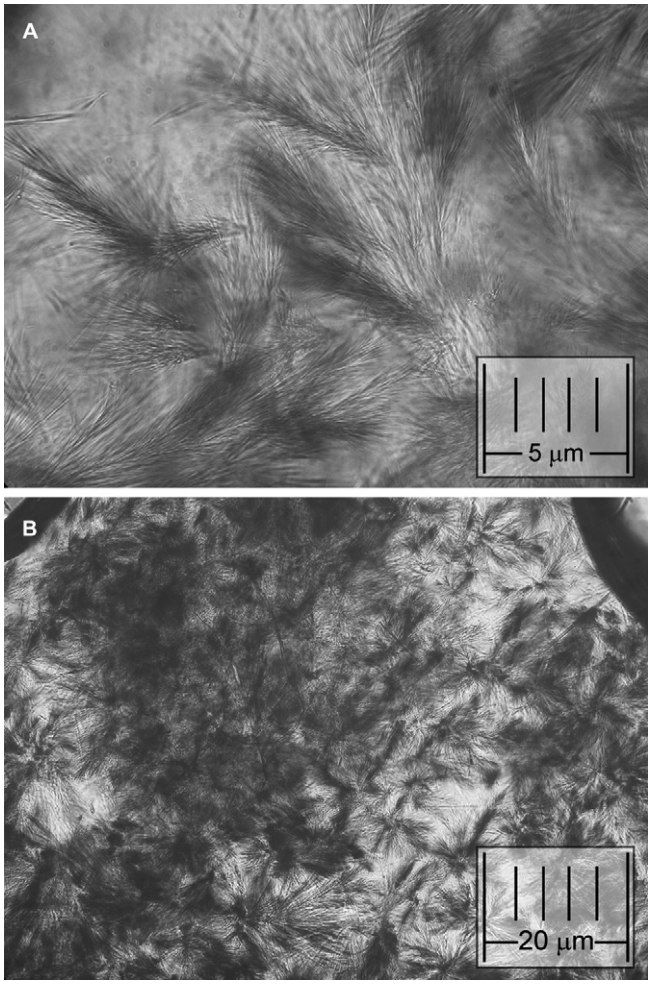

Fig. 7. Polarized Optical Microscopy micrographs of benzene gel **1** [2%(wt %)]: high magnification (A) and low magnification (B).

The hydrogen bond interaction is responsible for one-dimensional growth of the fibers along the fibril axes. The van der Waals interactions (much smaller) are responsible for the growth perpendicular to the fibril axes and make the fibril thicker.

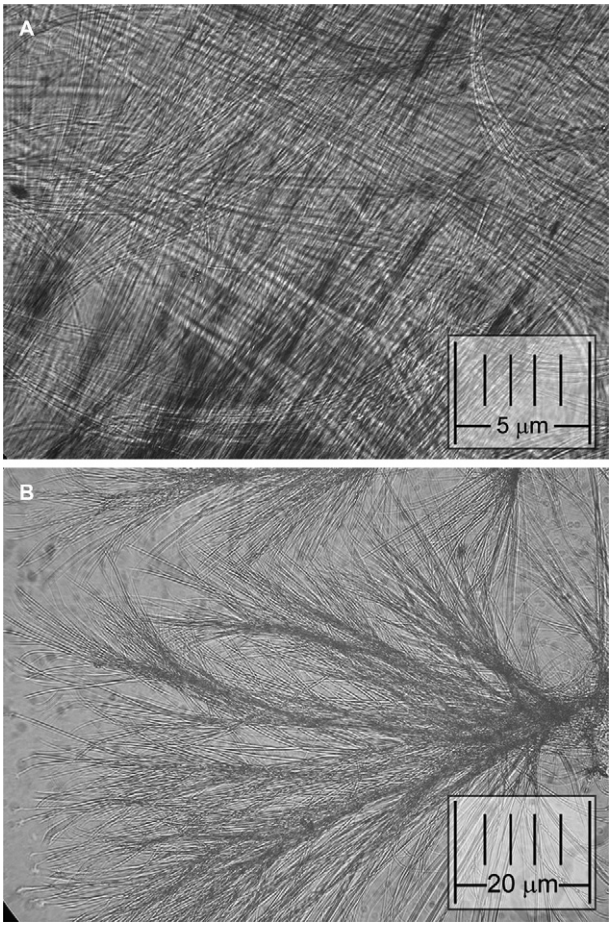

Fig. 8. Polarized Optical Microscopy micrographs of chlorobenzene gel **1** [2%(wt %)]: high magnification (A) and low magnification (B).

Such an interaction may play some role in the toluene gel where the fibrils are thicker when compared to other gels. As proved by FTIR measurements, the hydrogen bonds are the main driving forces for molecular aggregation in benzene, toluene, and chlorobenzene gels. Despite the common driving forces gelator **1** forms different aggregates in the gels made with these solvents. Therefore, we can conclude that the physical properties of the solvent, not the gelator–gelator interactions, have a decisive effect on the shape of the formed gelator aggregates in the gel.

2.4. Solvent influence

There is an effect of the nature of the solvent on the thermal stability of the gels of **1** and the aggregates' structures. In the literature different approaches have been used to quantify solvent effects employing solvent parameters, such as dielectric constant (ε), the one-component solubility parameter (δ), the polarity parameter $E_T(30)$ or the Kamlet–Taft parameters.[32–38] For selected solvents these parameters are given in Table 2. The δ parameter does not reflect the gelator–solvent molecular interactions but indicates the solvation power of the solvent toward gelator molecules and, thus, influences gelation. The solvent–gelator interactions are described by the $E_T(30)$ parameter and Kamlet–Taft parameters such as hydrogen bond donor ability (α), hydrogen bond acceptor ability (β), and solvent dipolarity/polarisability (π^*). The attempts to correlate the macroscopic properties of gelation to these parameters of solvent are in some cases satisfactory but why some correlation occurs is not fully understood.[32–38]

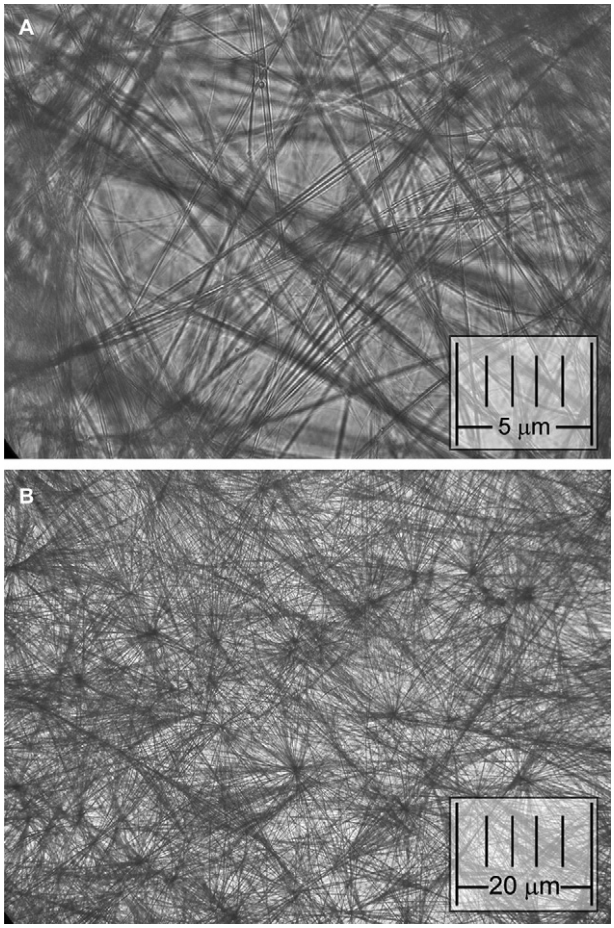

Fig. 9. Polarized Optical Microscopy micrographs of water hydrogel **1** [2%(wt %)]: high magnification (A) and low magnification (B).

We could expect that in a polar medium the gelation slows down due to the competing interactions with gelator molecules. This effect should also reduce the gel formation and dissolution temperature. The dielectric constants, which somehow reflect the solvent polarity of selected nonpolar solvents have much smaller values (between 2.2 and 5.6) than the polar solvents (17.8 and 80.6). Despite this fact gels composed of gelator **1** with all selected solvents are characterized by very similar (with the exception for butanol gel) gel–sol phase transition temperature. Therefore, we can conclude that there is no correlation between the ε quantity and T_{gel} for the studied gels.

Some correlation may be observed between the dielectric constant and the melting enthalpy ΔH. For nonpolar solvents the enthalpy values decreases with an increase of the ε values, whereas this behavior is opposite in the case of polar solvents. The similar correlation is observed for the solubility parameters δ and the polarity parameter $E_T(30)$ for both types of selected solvents.

Further, we have considered the effect of the selected solvents on the gelation of **1** in terms of Kamlet–Taft parameters. The solvents with α equal zero, such as toluene, benzene, and chlorobenzene, which are unable to donate bonds to the gelator formed with gelator **1** an optically completely clear gel. This means that the aggregates are smaller than the wavelengths of visible light. On the other hand, water with the highest value of α formed an opaque gel indicating the presence of large aggregates with a size comparable with the wavelengths of visible light. Water is a good hydrogen bond donor and can form hydrogen bonds with the gelator giving rise to the growth of the hydrogen-bonding network of gelator molecules in all directions. As a result larger aggregates are formed. Also water, being a good hydrogen donor, does not support gelation of **1** at low concentration. A stable hydrogel was obtained at concentration of 1.5% of gelator **1** contrary to nonpolar solvents, which formed stable gels for concentration less than 0.5% [wt %]. A similar situation arises with the butanol gel with gelator **1**. In the group of polar solvents the highest thermal stability is observed for glycerol gel of **1**. Glycerol has a high π^* and intermediate value of β among selected polar solvents. Glycerol can compete with the gelator–gelator interactions but despite that formed the most thermally stable gel. Within the nonpolar solvents the most thermally stable gel of **1** is formed in chlorobenzene, which has the lowest β and highest π^* values among the selected solvents of this type.

Generally, for the sugar-based gelator methyl-4,6-*O*-(*p*-nitrobenzylidene)-α-D-glucopyranoside, the correlation between the thermal stability and the Kamlet–Taft parameters π^* and β are different than for the family of bis-urea based gelators.[38] According to the studies by Smith et al.[38] the 1,2-dichlorobenzene with the parameters π^* and β (0.77 and 0.03, respectively) very similar to chlorobenzene, formed with bis-urea based gelators a less thermally stable gel when compared to toluene and benzene. This means that the attempt to correlate the Kamlet–Taft parameters to the thermal stability and gelation ability is possible but applies only for specified family of LMOGs. In our studies the correlation between the Kamlet–Taft parameters and the thermal stability and gelation ability of the studied gels was drawn on the basis of a limited number of solvents and therefore should be taken with some caution.

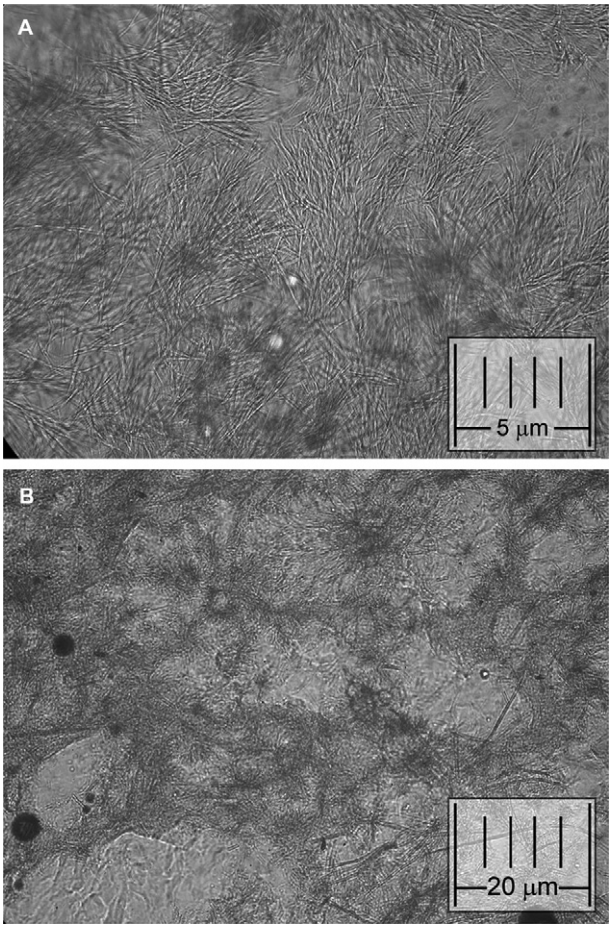

Fig. 10. Polarized Optical Microscopy micrographs of glycerol gel **1** [2%(wt %)]: high magnification (A) and low magnification (B).

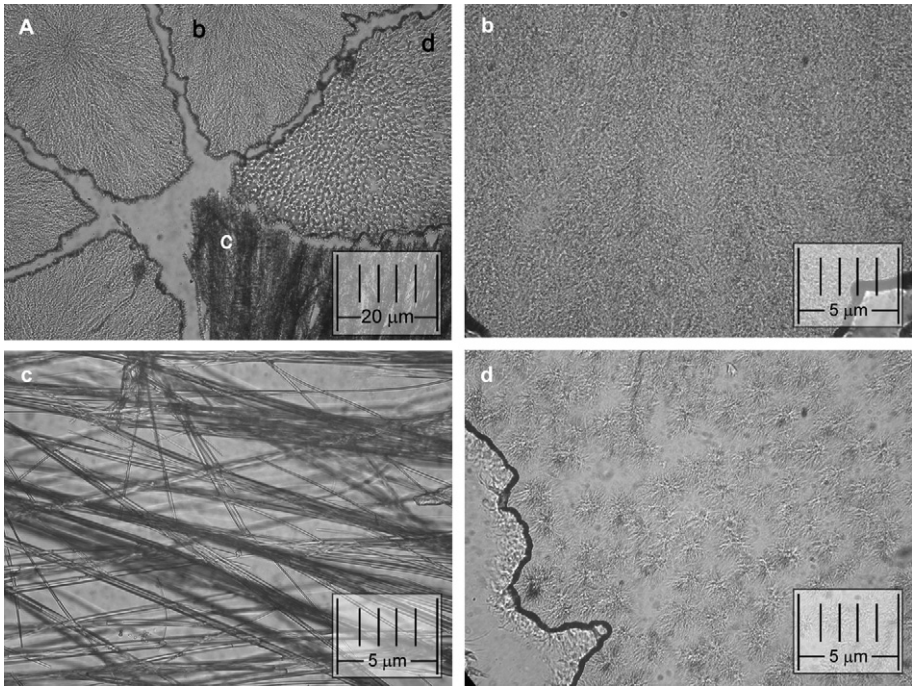

Fig. 11. Polarized Optical Microscopy micrographs of butanol gel **1** [3%(wt %)]: low magnification of gel microstructure (A), high magnification of microstructure (b), (c), and (d). The symbols correspond to that from Fig. 11A.

3. Conclusion

This work indicates the evident responsibility of the solvents to determine the supramolecular structure in the gels of methyl-4,6-*O*-(*p*-nitrobenzylidene)-α-D-glucopyranoside, their thermal stability, and their ability to form gels at low concentration. We have shown that some correlations of the physical properties of the solvents, such as dielectric constant, the one-component solubility, and the polarity parameter to the gel–sol transition temperature and to the calculated enthalpy of the phase transition occur but are not satisfactory. Moreover, the effort to correlate the Kamlet–Taft parameters to the thermal stability and gelation ability is also possible but applies only to the studied LMOGs. The correlations are different when compared to these obtained for bis-urea based gelators.[38]

We have shown that the driving forces for the aggregation of gelator **1** molecules in the chosen nonpolar solvents are the intermolecular hydrogen bonds like in other sugar-based gelator. The interesting results concern the fact that also in polar solvents this interaction is the main driving force of gelator self-assembly. Other aggregation modes, such as dipole–dipole, hydrophobic or π–π stacking interactions may play some role in the self-assembly of gelator **1** in the polar solvents.

The results presented in the paper indicate how complex the gelation phenomenon is and how unpredictable the influence of solvent on the gelation is.

4. Experimental section

4.1. Gelator and solvents

LMOG methyl-4,6-*O*-(*p*-nitrobenzylidene)-α-D-glucopyranoside (**1**) was synthesized according to a method described elsewhere.[26] The unique feature of this gelator is that it has the ability to gelate various organic solvents but also polar solvent like water or alcohols. In our work we examine the gelation ability of **1** in six different solvents: toluene, benzene, chlorobenzene, butanol, glycerol, and water. The solvents were obtained commercially from the Aldrich Chemical Co. and were used as supply.

4.2. Preparation of the gels

The methyl-4,6-*O*-(*p*-nitrobenzylidene)-α-D-glucopyranoside can gelatinize solvents in a wide range of concentration. The concentrations in the range 0.5%–6% [wt %] were chosen to form gels studied in the present work. The studied gelator made gels with all selected solvents but in different ranges of concentrations. The gels were prepared by mixing the required amount of the methyl-4,6-*O*-(*p*-nitrobenzylidene)-α-D-glucopyranoside and appropriate solvent in a closed capped tube and heating the mixture until the complete dissolution of the solid. Next, after cooling the solution below the characteristic gelation temperature the transition to the gel phase takes place. As a result thermoreversible, optically completely clear gels were obtained for benzene, chlorobenzene, and toluene. The gels obtained for glycerol and water were less clear and opaque. All gels kept stable even when the tubes were turned upside down, indicating the formation of stable supramolecular gels or hydrogels.

4.3. Determination of gel–sol transition temperature (T_{gel})

Thermal stabilities of the gels were analyzed by the air-bath method and visual inspection of the samples. The air-bath method involves inserting a sample into a stream of continuous gas flow, whose temperature changes are precisely controlled. For this purpose, we used a slightly modified NMR probe head. The opaque radio-frequency coil was replaced by a transparent glass tube, and thus, a visual inspection of the sample was possible. The temperature of the gel–sol (T_{gel}) transition was determined upon heating the sample to the temperature at which the system starts to flow and was measured with an accuracy of ±0.5 K.

4.4. FTIR Spectroscopy

FTIR measurements were performed on a Bruker Equinox 55 spectrometer. The absorption spectra of solvents, powdered gelator and its gels were obtained at room temperature in the range of 800–3600 cm^{-1} and a resolution of 2 cm^{-1}. The measured samples were dispersed in KBr pellets. To avoid any trace of water in KBr discs, as this substance is highly hydrophilic, the KBr powder used for the discs' preparation was kept under high temperature for a couple of hours. Next, the FTIR spectrum of this powder was measured. For the preparation of samples with our gelator we used only a freshly prepared and well dried KBr powder (without water bands in its FTIR spectra). To check the possible absorption of water by the KBr disc with our sample during the FTIR measurements, a pure KBr disc without gelator was kept in the same conditions and for the same period of time. Directly after our sample measurement, the spectrum of the pure disc was performed and checked for the existence of water bands.

4.5. Microscopic observation

Polarized Optical Microscopy (POM) investigation was performed with a JENAPOL microscope operating in different contrast and polarization modes. A drop of 3 or 2%(wt %) of methyl-4,6-*O*-benzylidene-α-D-glucopyranoside gels were carefully cast onto glass microscope slides and covered with 130–170 μm coverslip and then immediately subjected to POM observation.

Acknowledgements

This work has been supported by funds from the National Centre for Science as research project N N202 1961 40.

References and notes

1. Luboradzki, R.; Pakulski, Z.; Sartowska, B. *Tetrahedron* **2005**, *61*, 10122–10128.
2. Luboradzki, R.; Pakulski, Z. *Tetrahedron* **2004**, *60*, 4613–4616.
3. Gronwald, O.; Snip, E.; Shinkai, S. *Curr. Opin. Colloid Interface Sci.* **2002**, *7*, 148–156.
4. Amanokura, N.; Kanekiyo, Y.; Shinkai, S.; Reinhoudt, D. N. *J. Chem. Soc., Perkin Trans. 2* **1999**, 1995–2000.
5. Tritt-Goc, J.; Bielejewski, M.; Luboradzki, R.; Łapiński, A. *Langmuir* **2008**, *24*, 534–540.
6. Bielejewski, M.; Łapiński, A.; Kaszyńska, J.; Luboradzki, R.; Tritt-Goc, J. *Tetrahedron Lett.* **2008**, *49*, 6685–6689.
7. Weiss, R. G.; Terech, P. *Molecular Gels, Materials with Self–Assembled Fibrillar Network*; Springer: Dordrecht, The Netherlands, 2006.
8. George, M.; Weiss, R. G. *Acc. Chem. Res.* **2006**, *39*, 489–497.
9. Estroff, L. A.; Hamilton, D. *Chem. Rev.* **2004**, *104*, 1201–1218.
10. Terech, P.; Weiss, R. G. *Chem. Rev.* **1997**, *97*, 3133–3159.
11. Llusar, M.; Sanchez, C. *Chem. Mater.* **2008**, *20*, 782–820.
12. Samai, S.; Dey, J.; Biradha, K. *Soft Matter* **2011**, *7*, 2121–2126.
13. Piepenbrock, M. O. M.; Lloyd, G. O.; Clarke, N.; Steed, J. W. *Chem. Rev.* **2010**, *110*, 1960–2004.
14. Jung, J. H.; John, G.; Masuda, M.; Yoshida, K.; Shinkai, S.; Shimizu, T. *Langmuir* **2001**, *17*, 7229–7232.
15. Liu, J. W.; Mab, J. T.; Chen, C. F. *Tetrahedron* **2011**, *67*, 85–91.
16. Roy, S.; Chakraborty, A.; Chattopadhyay, B.; Bhattacharya, A.; Mukherjee, A. K.; Ghosh, R. *Tetrahedron* **2010**, *66*, 8512–8521.
17. Goyal, N.; Cheuk, S.; Wang, G. *Tetrahedron* **2010**, *66*, 5962–5971.
18. Bielejewski, M.; Tritt-Goc, J. *Langmuir* **2010**, *26*, 17459–17464.
19. Kowalczuk, J.; Jarosz, S.; Tritt-Goc, J. *Tetrahedron* **2009**, *65*, 9801–9806.
20. Tritt-Goc, J.; Bielejewski, M.; Luboradzki, R. *Tetrahedron*, **2011**, submitted for publication.
21. Luboradzki, R.; Gronwald, O.; Ikeda, M.; Shinkai, S.; Reinhoudt, D. N. *Tetrahedron* **2000**, *56*, 9595–9599.
22. Gronwald, O.; Shinkai, S. *Chem.—Eur. J.* **2001**, *7*, 4328–4334.
23. Luboradzki, R.; Gronwald, O.; Ikeda, M.; Shinkai, S. *Chem. Lett.* **2000**, *X*, 1148–1149.
24. Lee, K. Y.; Mooney, D. J. *Chem. Rev.* **2001**, *101*, 1869–1879.
25. Miyata, T.; Uragamia, T.; Nakamach, K. *Adv. Drug Delivery Rev.* **2002**, *54*, 79–98.
26. Gronwald, O.; Shinkai, S. *J. Chem. Soc., Perkin Trans. 2* **2001**, 1933–1937.
27. Murata, K.; Aoki, K.; Suzuki, T.; Hanada, T.; Kawabata, H.; Komori, T.; Oseto, F.; Ueda, K.; Shinkai, S. *J. Am. Chem. Soc.* **1994**, *116*, 6664–6674 and references cited therein.
28. Garner, C. M.; Terech, P.; Allegraud, J. J.; Mistrot, B.; Nguyen, P.; de Geyer, A.; Rivera, D. *J. Chem. Soc., Faraday Trans.* **1998**, *94*, 2173–2179.
29. Gronwald, O.; Sakurai, K.; Luboradzki, R.; Kiura, T.; Shinkai, S. *Carbohydr. Res.* **2001**, *331*, 307–318.
30. Yoza, K.; Ono, Y.; Yoshihara, K.; Akao, T.; Shinmori, H.; Takeuchi, M.; Shinkai, S.; Reinhoudt, D. N. *Chem. Commun.* **1998**, 907–908.
31. Yoza, K.; Amanokura, N.; Ono, Y.; Akao, T.; Shinmori, H.; Takeuchi, M.; Shinkai, S.; Reinhoudt, D. N. *Chem.—Eur. J.* **1999**, *5*, 2722–2729.
32. Makarevic, J.; Jokic, M.; Peric, M.; Tomisic, V.; Kojic-Prodic, B.; Zinic, M. *Chem.—Eur. J.* **2001**, *7*, 3328–3341.
33. Bielejewski, M.; Łapiński, A. ;; Luboradzki, R.; Tritt-Goc, J. *Langmuir* **2009**, *25*, 8274–8279.
34. Zhu, G.; Dordic, J. S. *Chem. Mater.* **2006**, *18*, 5988–5995.
35. Hanabusa, K.; Matsumoto, M.; Kimura, M.; Kakehi, A.; Shirai, H. *J. Colloid Interface Sci.* **2000**, *224*, 231–244.
36. Hirst, A. R.; Smith, D. *Langmuir* **2004**, *20*, 10851–10857.
37. Kamlet, M. J.; Abbound, L. M.; Abraham, M. H.; Taft, R. W. *J. Org. Chem.* **1983**, *48*, 2877–2887.
38. Edwards, W.; Lagadec, C. A.; Smith, D. K. *Soft Matter* **2011**, *7*, 110–117.